Available online at www.sciencedirect.com
ScienceDirect
Tetrahedron
Tetrahedron 63 (2007) 1695–1705

New star-shaped triarylamines: synthesis, mesomorphic behavior, and photophysical properties

Yueh-Ju Wang,[a] Hwo-Shuenn Sheu[b] and Chung K. Lai[a,*]

[a]*Department of Chemistry and Center for Nano Science Technology, UST, National Central University, Chung-Li 32054, Taiwan, ROC*
[b]*National Synchrotron Radiation Research Center, Hsinchu 30077, Taiwan, ROC*

Received 14 August 2006; revised 9 November 2006; accepted 10 November 2006
Available online 22 December 2006

Abstract—A total of 18 compounds **1**–**6** derived from triphenylamine as core group were prepared and characterized, and their mesomorphic properties were also investigated. Compounds **1**–**4** and **5**,**6** were prepared from *p*,*p*′,*p*″-triformyltriphenylamine and *p*,*p*′-diformyltriphenylamine with appropriate alkoxyphenylamines. The phase behavior of these mesogenic compounds was characterized and studied by differential scanning calorimetry, polarized optical microscopy, and powder XRD diffraction. Compounds **1**–**3** exhibited columnar mesophase, however, compounds **4**–**6** were nonmesogenic. The mesophases observed in compounds **1**–**3** were found to be side dependent. Compounds **1a**, **2a**, and **3a** appended with one, two, or three side chains exhibited lamellar columnar (Col_L) phases, and compounds **2b** and **3b** with four or six side chains formed hexagonal columnar (Col_h) phases. The formation of the mesophases, lamellar or columnar mesophases, was probably induced by H-bonding formed between $-CH_2NH$ groups. The oxidation process determined by cyclic voltammetry showed two redox waves, one appeared at 220–255 mV and the other one at 503–677 mV, which gave energy to HOMOs range of 5.02–5.36 eV. The fluorescent properties of the compounds were examined. All λ_{max} peaks of the absorption and photoluminescence spectra of compounds occurred at ca. 307–392 nm and 368–456 nm, respectively. Compound **4a** has a larger red shift due to a better conjugation linked by C=C double bonds instead of $-CH_2NH$ in other compounds.

1. Introduction

Liquid crystalline materials[1] have been found attractive in terms of possessing both self-organizing capability and fluidity, and these properties make them as excellent potential candidates in device applications. Among them discotic molecules, as a fairly new category, were often generated by adding long hydrocarbon tails to a flat core. The formation of discotic or columnar mesophase by round or discotic molecules was often found to be side chain dependent. On the other hand, more side chains are generally needed for larger core centers in order to stabilize the mesogens. A few mesophases, such as hexagonal (Col_h), rectangular columnar (Col_r), lamellar columnar (Col_L), or nematic columnar (Col_N), were commonly observed. A transition[2] between these phases, for example, $Col_h \rightarrow Col_r$ or $Col_h \rightarrow Col_N$, was occasionally observed, and these phase transitions were all related to the temperature dependency or/and side chain length dependency of compounds. This type of molecules is capable of stacking spontaneously into individual molecular columns behaving electronically as one-dimensional molecular wires.[3]

During the past years organic electroluminescence[4] (EL) has been attracting considerable interest as a technology used in the display applications. However, the efficiency until today is in fact limited due to their crystallization. Therefore, new materials with a high degree of molecular orientation then expect some advantages.[5] Charge transport occurred within the active layers in a device has been truly vital to the EL devices. Charge carriers cannot travel over extended distances along the main chain since the flexible spacers break the conjugation of the backbone. The stacking of mesogenic units into a column or smectic layer rather than a nematic phase was long known to improve carrier mobility,[6] which offers an excellent approach to the problem. These high electronic properties associated with long range columnar order make discotic liquid crystals promising as organic semiconductors for applications in the domain of molecular electronics and optoelectronics,[7] more particularly, in the area of photoconductivity and for photovoltaic and electroluminescent devices. Though photophysical and electronic studies[8] have been investigated, yet there still remains much to be learned from the analysis of the photophysics of these liquid crystalline materials. On the other hand, the use of arylamines[9] as hole-transporting molecules within organic light emitting diodes (OLED) has been well documented. Amorphous but not liquid crystalline materials were often obtained due to their nonplanar conformations.[10]

* Corresponding author. Tel.: +886 03 4259207; fax: +886 03 4277972; e-mail: cklai@cc.ncu.edu.tw

0040–4020/$ - see front matter © 2006 Elsevier Ltd. All rights reserved.
doi:10.1016/j.tet.2006.11.058

Therefore, preparing liquid crystals by use of nonplanar triphenylamines as core become a true challenge.

In this work, we describe herein the preparation, mesomorphic and photophysical studies of a new type of discotic molecules derived from triphenylamine. These compounds showed a strong dependence on the formation of the mesomorphic properties. Compounds **1a**, **2a**, and **3a** with one, two, and three side chains formed lamellar (Col_L) phases, and compounds **2b** and **3b** exhibited hexagonal columnar (Col_h) phases. However, all other compounds **4**–**6** formed crystal phases. This is probably the first example of triphenylamine-based derivatives exhibiting columnar phases. Their fluorescent properties as well as electrochemical behavior were also examined as potential application in hole-transporting materials.

2. Results and discussion

2.1. Synthesis and characterization

The synthetic pathways for compounds **1**–**6** are summarized in Schemes 1 and 2. The formylation of triphenylamine with $POCl_3$ (10 equiv) in *N*,*N*-dimethylformamide (>10 equiv) gave a mixture of *p*,*p*′,*p*″-triformyltriphenylamine[11] and *p*,*p*′-diformyltriphenylamine with a yield of 10% and 42%, respectively. Monosubstituted *p*-formyltriphenylamine was not obtained in this reaction conditions, and those two compounds were easily separated and purified by flash chromatography (silica gel). The two substituted triphenylamines were then used to prepare all other derivatives in this work. *p*,*p*′-Diformyltriphenylamine was further reacted with 4-alkoxyphenylamines or 3,4-dialkoxyphenylamines in refluxing absolute ethanol to give Schiff bases as precursors for compounds **5a** and **5b**, and the Schiff bases prepared as intermediates were not isolated in this study. Compounds **5a** and **5b** were obtained by the reduction of these Schiff bases with $NaBH_4$ stirred in THF/CH_3OH. A characteristic singlet appeared at 4.20–4.25 ppm, assigned to $–NCH_2$ group, was used to characterize the products. Compound **6a** was similarly prepared from 4-bromophenyl-bis-(4-formylphenyl)amine, which was obtained by bromination with Br_2. A mixture of compounds **1a**, **2a**, and **3a** was obtained by Schiff bases' condensation reaction with 1 equiv of *p*,*p*′,*p*″-triformyltriphenylamine and 2 equiv of alkoxyphenylamine, followed by in situ reduction with $NaBH_4$. Then compounds **1a**, **2a**, and **3a** were separated and purified by flash chromatography (silica gel) by eluting with hexane/ethyl acetate (4/1). A yield of 8%, 41–48%, and 19–23% was obtained for compounds **1a**, **2a**, and **3a**, respectively. These imine Schiff bases as precursors for final compounds were slightly difficult to purify or separate. Therefore, all Schiff bases were directly further reduced by $NaBH_4$ without any purification. Compounds **2b** and **3b** were prepared similar to compounds **1a**, **2a**, and **3a**. All final compounds were isolated as white to pale yellow solids or pastes depending on the carbon length attached. All intermediates and products were identified and characterized by ^1H and ^{13}C NMR spectroscopies and elemental analysis.

2.2. Mesomorphic properties

The mesomorphic behavior of compounds **1**–**6** was studied by differential scanning calorimetry (DSC) and polarized optical microscopy. The phase transitions and thermodynamic data of compounds **1**–**6** are summarized in Table 1. The mesomorphic results indicated that compounds

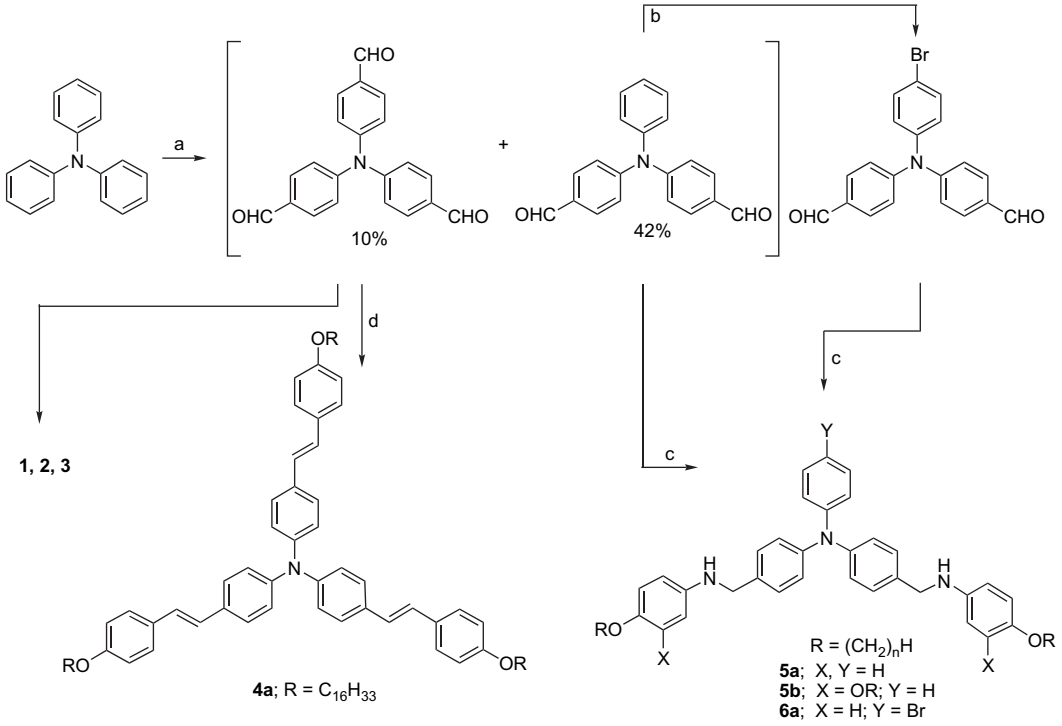

Scheme 1. Reagents and conditions: (a) $POCl_3$ (10.0 equiv), DMF (10.0 equiv), 100 °C, 72 h; (b) Br_2 (1.0 equiv) in CH_2Cl_2, 35 °C, 2 h, 95%; (c) 4-alkoxyphenylamines or 3,4-alkoxyphenylamines (2.0 equiv), trace HOAc in absolute ethanol, reflux 24 h, then $NaBH_4$ (4.0 equiv), stirred in THF/MeOH, 4 h, 60–77%; (d) alkoxybenzyltriphenylphosphonium bromide (3.0 equiv), KO(*t*-Bu) (1.2 equiv), refluxed in dry THF, 48 h, 19%.

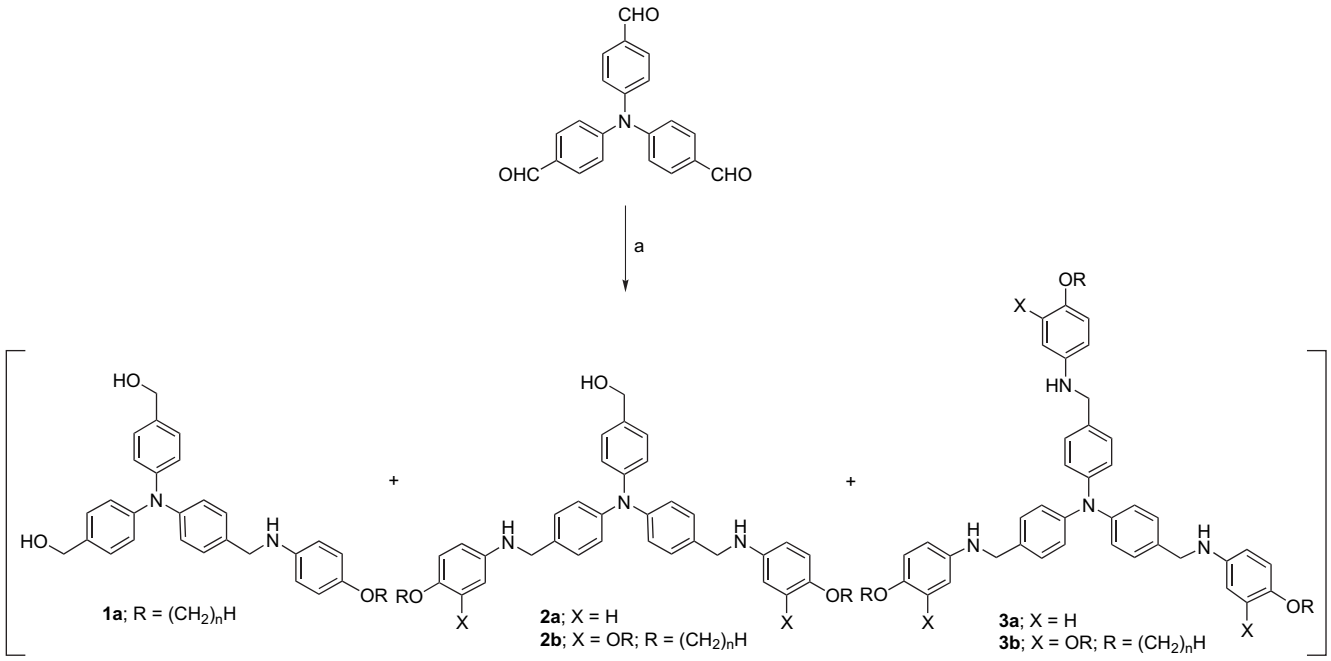

Scheme 2. Reagents and conditions: (a) 4-alkoxyphenylamines or 3,4-alkoxyphenylamines (2.0 equiv), trace HOAc in absolute ethanol, reflux 24 h, then $NaBH_4$ (6.0 equiv), stirred in THF/MeOH, 4 h. Yield: 8% (**1**), 41–48% (**2**), and 19–23% (**3**).

1a, **2a**, and **3a** exhibited lamellar columnar (Col_L) phases. As can be seen from the table, the formation of mesophases observed was strongly dependent on the side chains or on the structure. Compounds **1a**, **2a**, and **3a** with a total of one, two, and three side chains appended exhibited lamellar columnar phase. These compounds appeared as white powders at room temperature. However, they melted into viscous phases upon slow heating. Upon DSC analysis all these compounds exhibited a typical transition behavior, and two enantiotropic transitions, crystal-to-mesophase (Cr→M) and mesophase-to-isotropic (M→I), were observed. Both the melting temperatures and the clearing temperature slightly decreased with side chains, i.e., 44.7 (**1a**)>26.8 (**2a**)~30.0 °C (**3a**) and 79.2 (**1a**)>57.7 (**2a**)>52.2 °C (**3a**) on heating cycle. Under the polarized optical microscope they all displayed fan-shaped textures (shown in Fig. 1) without homeotropic behavior observed, therefore, the mesophase was characterized and identified as lamellar columnar (Col_L) phase. The temperature range of the lamellar phases was in fact quite narrow, in the range of 34.5 (**1a**)>30.9 (**2a**)>22.2 °C (**3a**) on heating. Interesting to note, the enthalpy involved in Col_L→I transitions increased with side chains, i.e., ΔH= 1.00 (**1a**)<2.88 (**2a**)<6.21 kJ/mol (**3a**), indicating a higher change in entropy by compound **3a** than **1a**. On cooling back to room temperature, compounds **2a** (n=14) and **3a** (n=14) formed frozen mesophases. In the series of homologues of compound **2a**, increasing the carbon chains (n= 14→18) increased both the clearing temperatures (26.8→ 54.9 °C) and the melting temperatures (57.7→68.6 °C). However, the temperature range of the mesophases was decreased with side chains, i.e., ΔT=30.9 (n=14)>25.6 (n=16)>13.7 °C (n=18). Figure 2 showed the bar graph of the transition temperature of compounds **1**–**6**. The formation of columnar phases was generally found to depend crucially on the side chain density. In general, the side chain density required for the columnar phases was strongly dependent on the size or the flexibility of the core center, i.e., the larger the size or the more rigid is the core group, more side chain density is often needed. The overall molecular shape of compound **1a** or **2a** is not a perfect discotic or round, and the side chains appended around the core triphenylamine might not also be enough to form a stable columnar phase. However, the formation of the columnar phase was possibly induced by neighboring molecules above and beneath. The force or interaction that induces the liquid crystalline phase in these compounds was believed to be the H-bonds (–$CH_2NH\cdots NHCH_2$) formed between the –CH_2NH groups. The representative scheme for the molecular stacking in the columnar phase is shown in Figure 3.

As the number of carbon chains of the compounds was increased to four (**2b**) or six (**3b**) alkoxy groups, the mesophase was better improved. The DSC analysis was similar to that of compound **2b**, and one typical DSC thermogram is shown in Figure 4. Compounds **2b** and **3b** exhibited hexagonal columnar phases, and the Col_h phase was also characterized by polarized optical microscope. A typically pseudo focal-conic texture (see Fig. 1) with linear birefringent defects on slow cooling from the isotropic liquid was clearly observed. This observed texture also accompanied by a large area of homeotropic domain is often characteristic of hexagonal columnar phases. In this series for compounds **2b** and **3b** forming Col_h phases, both melting temperatures and clearing temperatures increased with carbon chain length, i.e., T_m=20.5 (n=12)<36.8 (n=14)<62.2 °C (n= 16) and T_{cl}=56.3 (n=12)<62.6 (n=14)<67.6 °C (n=16) for compound **2b** versus T_m=26.6 (n=10)<32.5 (n= 12)<49.8 °C (n=14) and T_{cl}=44.2 (n=10)<52.7 (n= 12)<60.0 °C (n=14) for compound **3b** on heating. The temperature range of Col_h phase observed for compound **2b** also decreased with carbon chain length, i.e., ΔT=35.8

Table 1. Phase transitions and enthalpies of compounds **1–6**

1a	n=16	$Cr \underset{29.8\,(12.0)}{\overset{44.7\,(18.3)}{\rightleftharpoons}} Col_L \underset{76.1\,(0.98)}{\overset{79.2\,(1.00)}{\rightleftharpoons}} I$
2a	14	$Cr \underset{27.9}{\overset{26.8}{\rightleftharpoons}} Col_L \underset{55.6\,(2.89)}{\overset{57.7\,(2.88)}{\rightleftharpoons}} I$
	16	$Cr \underset{34.8\,(25.8)}{\overset{39.8\,(30.5)}{\rightleftharpoons}} Col_L \underset{63.8\,(3.30)}{\overset{65.4\,(3.27)}{\rightleftharpoons}} I$
	18	$Cr \underset{49.8\,(52.1)}{\overset{54.9\,(55.9)}{\rightleftharpoons}} Col_L \underset{67.6\,(2.13)}{\overset{68.6\,(2.06)}{\rightleftharpoons}} I$
2b	12	$Cr \overset{20.5}{\rightleftharpoons} Col_{hd} \underset{53.2\,(1.39)}{\overset{56.3\,(1.41)}{\rightleftharpoons}} I$
	14	$Cr \underset{26.2\,(14.1)}{\overset{36.8\,(15.5)}{\rightleftharpoons}} Col_{hd} \underset{60.4\,(4.51)}{\overset{62.6\,(2.43)}{\rightleftharpoons}} I$
	16	$Cr \underset{47.0\,(54.6)}{\overset{62.2\,(39.1)}{\rightleftharpoons}} Col_{hd} \underset{65.4\,(2.45)}{\overset{67.6\,(2.63)}{\rightleftharpoons}} I$
3a	14	$Cr \underset{29.8}{\overset{30.0}{\rightleftharpoons}} Col_L \underset{51.6\,(6.59)}{\overset{52.2\,(6.21)}{\rightleftharpoons}} I$
	16	$Cr \underset{41.8\,(15.6)}{\overset{44.9\,(18.8)}{\rightleftharpoons}} Col_L \underset{58.5\,(6.03)}{\overset{59.4\,(5.64)}{\rightleftharpoons}} I$
	18	$Cr \underset{51.5\,(34.7)}{\overset{54.1\,(39.1)}{\rightleftharpoons}} Col_L \underset{60.6\,(3.48)}{\overset{62.1\,(3.42)}{\rightleftharpoons}} I$
3b	10	$Cr \underset{22.6}{\overset{26.6}{\rightleftharpoons}} Col_{hd} \underset{34.8\,(1.90)}{\overset{44.2\,(2.86)}{\rightleftharpoons}} I$
	12	$Cr \underset{28.1\,(45.8)}{\overset{32.5\,(47.5)}{\rightleftharpoons}} Col_{hd} \underset{49.9\,(4.52)}{\overset{52.7\,(4.53)}{\rightleftharpoons}} I$
	14	$Cr \underset{37.8\,(83.4)}{\overset{49.8\,(84.2)}{\rightleftharpoons}} Col_{hd} \underset{57.1\,(4.15)}{\overset{60.0\,(4.24)}{\rightleftharpoons}} I$
	16	$Cr \underset{54.9\,(145.0)}{\overset{63.5\,(143.0)}{\rightleftharpoons}} I$
4a	16	$Cr_1 \underset{105.6\,(5.83)}{\overset{116.1\,(4.32)}{\rightleftharpoons}} Cr_2 \underset{133.6\,(50.5)}{\overset{139.4\,(48.7)}{\rightleftharpoons}} I$
5a	16	$Cr \underset{38.4\,(48.1)}{\overset{47.6\,(47.2)}{\rightleftharpoons}} I$
5b	16	$Cr \underset{38.1\,(129)}{\overset{47.8\,(129)}{\rightleftharpoons}} I$
6a	16	$Cr \underset{28.9\,(50.4)}{\overset{36.7\,(51.1)}{\rightleftharpoons}} I$

n represents the number of carbons in the alkoxy chain. Cr=crystal phases; Col_L=lamellar phase; Col_{hd}=disordered hexagonal columnar phase; I=isotropic. The transition temperatures (°C) and enthalpies (in parentheses, kJ/mol) are determined by DSC at a scan rate of 10.0 °C/min.

(n=12)>25.8 (n=14)>5.40 °C (n=16). However, this decreasing trend in temperature range of Col_h phases was not observed in compound **3b** (also see Fig. 2). All other compounds **4–6** were in fact nonmesogenic. Compound **4a** formed a crystal phase, and a direct transition of Cr→I phase at 139.4 °C was observed. The higher melting occurred at 139.4 °C also caused a better packing and/or a more π–π interaction between the phenyl groups. The lack of mesophases observed for compound **4a** might be possibly two-fold; one is the weak force or interaction to induce and the other one is the relative rigidity caused by shape effect. The first one was attributed to an incapability in forming H-bonding because of the C=C double bonds linked between the two phenyl groups. On the other hand, a more rigid sp^2-hybrid orbital in C=C bonds instead of a more flexible sp^3-hybrid orbital in CH_2NH bonds might also explain the formation of the crystal phases. Compounds **5a** and **5b** exhibited crystal phases regardless of the side chain density, and they all displayed a similar transition of Cr→I phase that occurred at 47.6 (**5a**) and 47.8 °C (**5b**). Incorporation of a larger dipole (compared to H) in compound **6a** resulted in a crystal phase. The lack of liquid crystallinity in compound **6a** might be attributed to the shape effect. The large size of Br atom might result in a difficult packing,

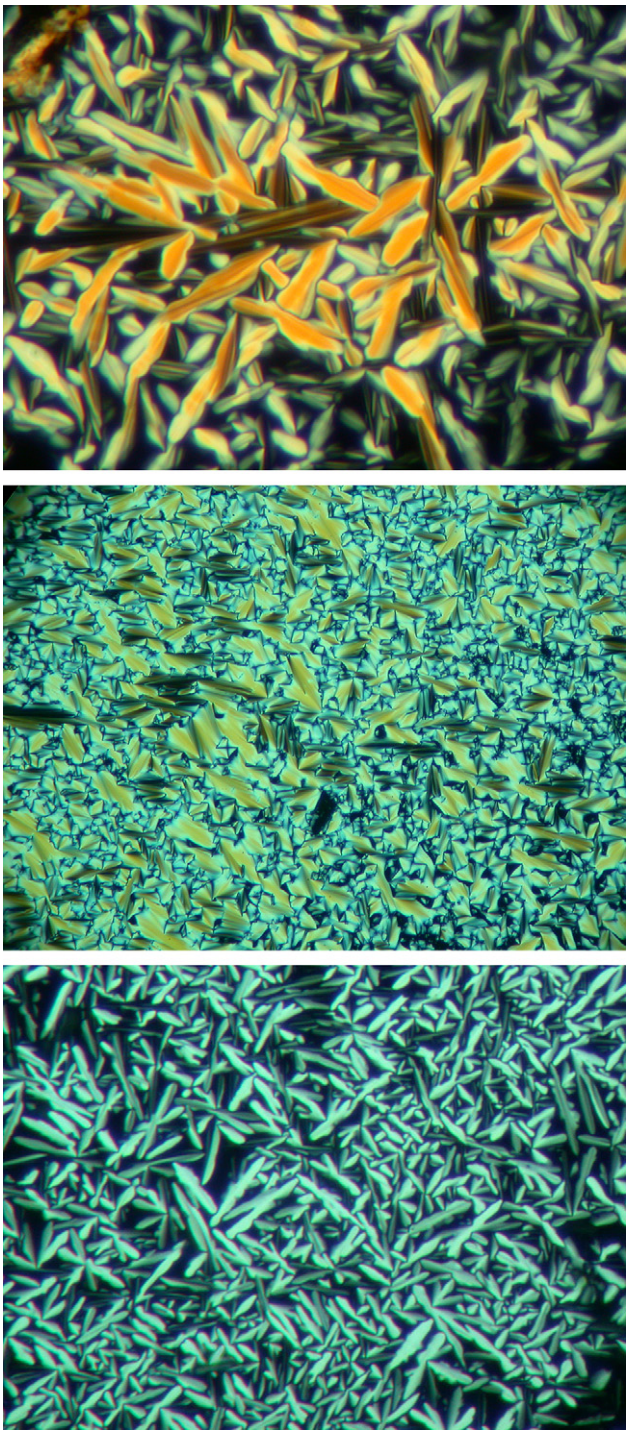

Figure 1. The optical textures observed for **2b** (n=16, top plate) at 60 °C, **3a** (n=16) at 55 °C, and **3b** (n=14, bottom plate) at 55 °C.

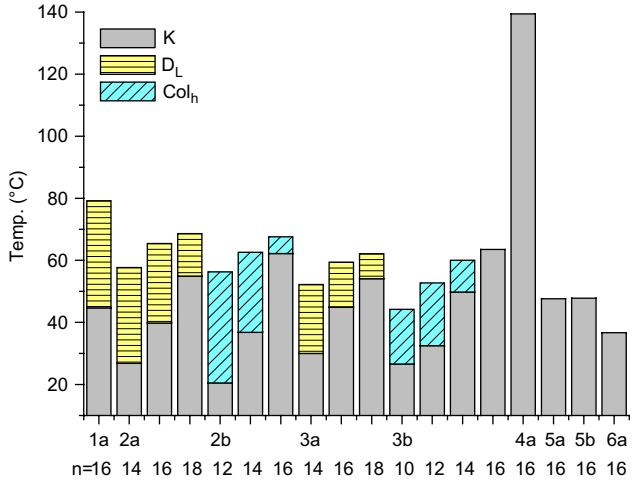

Figure 2. Bar graph showing the phase behavior of compounds **1**–**6**.

which was reflected to a lower melting temperature that occurred at 36.7 °C.

2.3. Variable temperature XRD diffraction

Variable temperature powder XRD diffraction was also used to confirm the structure of the mesophases. A summary of the diffraction peaks and lattice for compounds **3a** (n=14) and **3b** (n=14) is listed in Table 2. For compound **3a**, only one strong diffraction peak at lower angle and one broad diffused peak at wide-angle were observed. For example, compound **3a** (n=14) gave a diffraction of a strong reflection at d 47.15 Å and a broad diffused peak at 4.52 Å. This type of diffraction pattern corresponded to lamellar phases (Col_L) and hexagonal columnar phases (Col_h). However, the phase was characterized as Col_L based on textures observed by optical microscope. The diffraction peak corresponding to Miller indices is 100. In other discotic systems, higher diffraction peaks indexed as 200, 300, and others were occasionally observed. However, compounds **3b** exhibited a different diffraction patterns. The compounds displayed the diffraction pattern of a two-dimensional hexagonal lattice

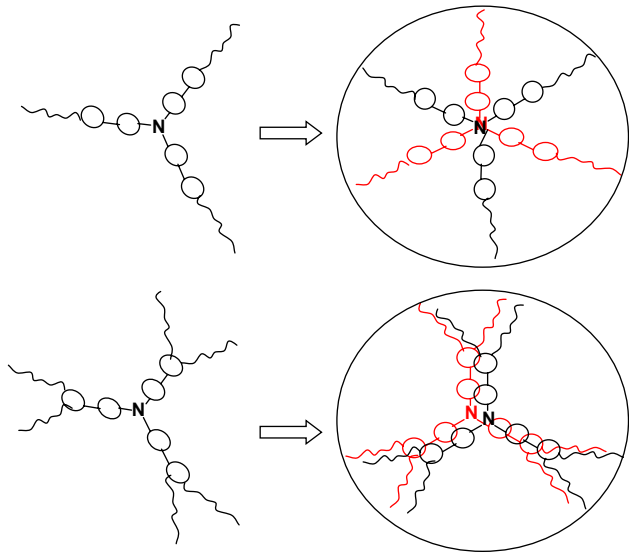

Figure 3. The schematic drawings of the molecules packed in columnar phases formed by compounds **3a** (top) and **3b** (bottom).

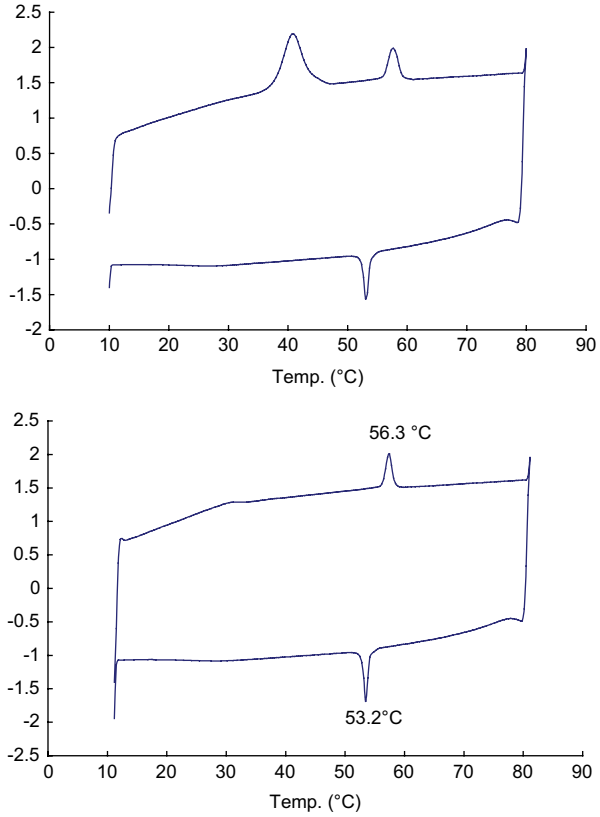

Figure 4. The DSC thermograms of compound **2b** (n=12) on first (top) and second cycles (bottom).

with one intensive peak and two weaker peaks. These are characteristic of columnar phases with a d-spacing ratio of 1, $(1/3)^{1/2}$, and $(1/4)^{1/2}$, corresponding to Miller indices 100, 110, and 200, respectively. For example, a diffraction pattern of an intense peak at 37.08 Å, 21.35 Å, 18.55 Å, and a broad diffused peak (4.51 Å) at wide-angle region was observed and this diffraction pattern corresponded to a hexagonal columnar arrangement. This pattern corresponds to an intercolumnar distance of 42.8 Å. This data were also quite consistent with the relatively small transition enthalpies of columnar-to-isotropic obtained by DSC analysis. A typical example of a diffraction pattern for compounds **3a** (n=14) and **3b** (n=14) phases is depicted in Figure 5.

2.4. Optical properties

The UV–vis absorption and PL spectra of compounds **1**–**6** in CH_2Cl_2 are presented in Figure 6. The data of λ_{max} peaks of UV–vis absorption and PL spectra in CH_2Cl_2 are listed in Table 3. The lowest energy absorptions of the compounds

Table 2. X-ray diffraction data of compounds **3a** and **3b**

Compound	Mesophase (temperature, °C)	Lattice constants (Å)	Spacing (Å)		Miller indices (hkl)
			d_{obsd}	d_{calcd}	
3a (n=14)	Col_L (45)	d=47.2	47.15	47.15	(001)
			4.52	—	Halo
3b (n=14)	Col_{hd} (45)	a=42.8	37.08	37.08	(100)
			21.35	21.41	(110)
			18.55	18.54	(200)
			4.51	—	Halo

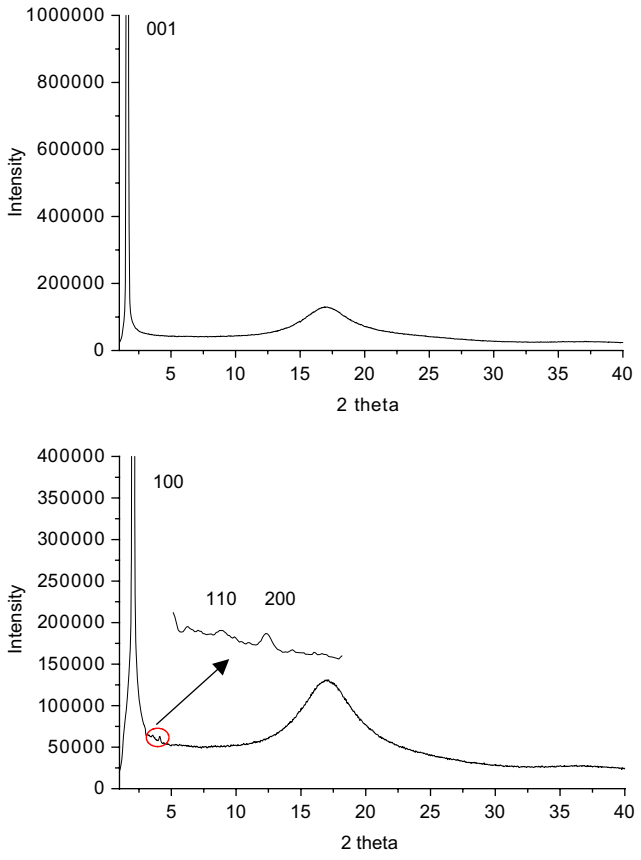

Figure 5. X-ray diffraction patterns of compound **3a** (n=14, top) at 45 °C and **3b** (n=14, bottom) at 45 °C.

are ranged in the region of 306–309 nm except for compound **4a**, which appeared at 392 nm. The larger red shift at ca. 83–86 nm was attributed to a longer or better conjugation. The electronic absorption energy of these compounds including Br-containing compound **6a** (except **4a**) is similar to UV–vis spectra. These compounds exhibited featureless emission, all displaying Stoke shifts at ca. 62–64 nm. All quantum yields (<1%) were quite lower except for compound **4a** (–55%). The lower quantum yields were attributed to the effect of the lone pair on the nitrogen atom. The lower fluorescence quantum efficiency of **6a** than that of **2** or **5** was attributed to the direct attachment of the bromine atom to the triphenylamine moiety, which led to a significant heavy atom effect.[12]

2.5. Electrochemistry

The redox propensity of these compounds was studied by cyclic voltammetry. In order to understand the effect of the redox properties on the structural moieties, compounds **1**–**6** with longer carbon side chains (n=16) were only investigated. The oxidation potentials measured in CH_2Cl_2 at room temperature and the derived orbital energies are given in Table 4. Two redox waves were observed; one was in the range of 220–255 mV and the other one was in the range of 503–677 mV. The first oxidation potentials were used to determine the HOMO energy levels. The energy of the HOMO of these materials was calculated with reference to ferrocene (4.8 eV) and ranged between 5.02 and 5.36 eV. Similarly, the optical edge was utilized to derive the band gap and the

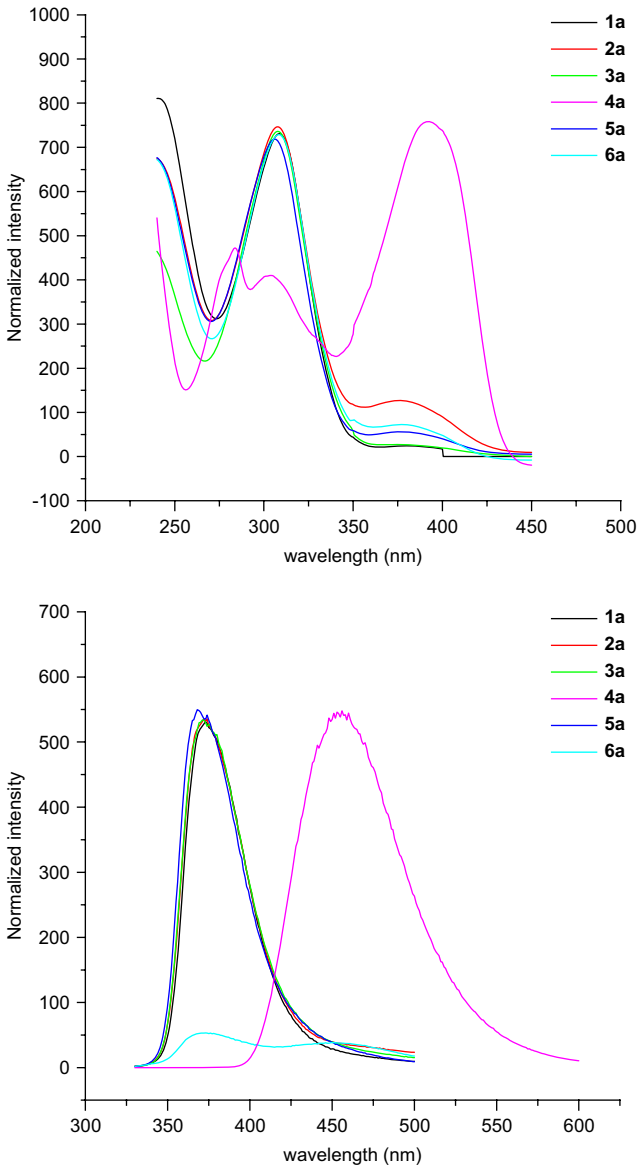

Figure 6. Absorption (top) and fluorescent spectra (bottom) of the compounds **1**–**6**.

LUMO energies. An interesting feature of the cyclic voltammetry of **3a** was the observation of one successive reversible one-electron redox process and an irreversible three-electron redox process (Fig. 7). The chemical stability of the electrogenerated intermediate was investigated by the applied scan rate. The oxidation processes were irreversible (220 mV) and pseudo-reversible (539 mV) at a scan rate of 0.1 V/s; however, both processes become more reversible at a scan

Table 3. Absorption and emission data of compounds **1a**–**6a**

Compd	λ_{max} (nm)	λ_{em} (nm)
1a (n=16)	309	373
2a (n=16)	308	372
3a (n=16)	308	372
4a (n=16)	392	456
5a (n=16)	306	368
6a (n=16)	307	373

Table 4. Electrochemical data and the derived orbital energies

Compd	E_{OX} (ΔE_P) (mV)	HOMO (eV)	LUMO (eV)	Band gap (eV)
1a (n=16)	231 (i), 503 (63)	5.03	1.38	3.65
2a (n=16)	230 (i), 550 (70)	5.03	1.38	3.65
3a (n=16)	220 (i), 539 (101)	5.02	1.37	3.65
4a (n=16)	564 (121)	5.36	2.54	2.82
5a (n=16)	235 (i), 593 (103)	5.04	1.39	3.65
6a (n=16)	255 (i), 677 (176)	5.06	1.41	3.65
TPA	540 (120)			

The scan rate was 100 mV/s^{-1}, TPA is triphenylamine, (i): irreversible.

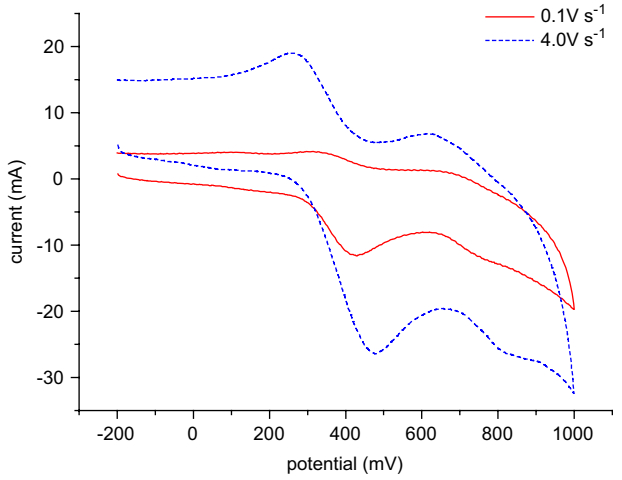

Figure 7. Cyclic voltammograms of **3b** (n=16) measured in CH_2Cl_2 at a scan rate of 0.1 V/s^{-1} and 4.0 V/s^{-1}.

rates higher than 4.0 V/s. This higher reversibility observed at higher scan rate might be attributed to the electrochemical instability of the cation or radical intermediate under the electrochemical condition. This is to say that the intermediate was observed more stable only at higher scan rate. Similar observations occurred in compounds **1a**, **2a**, **5a**, and **6a**. However, an irreversible two-electron redox for compounds **2a**, **5a**, and **6a**, and an irreversible one-electron redox for compound **1a** were observed. Based on these electrochemical data, the redox waves appeared in the range of 503–677 mV and 220–255 mV were assigned to the triphenylamine and the methylphenylamine moieties, respectively. In order to confirm the redox position, the TPA was also examined and its oxidation potential appeared at ca. 540 mV. In compound **3a**, the three methylphenylamines are not conjugated. On the other hand, all three methylphenylamines are structurally independent, and the oxidation process in fact occurred at the same time. As expected, compound **4a** has a lower LUMO energy because of the conjugation, which decreased the excitation energy level. The second oxidation becomes more difficult at 84 mV (i.e., 677 mV for compound **6a** to 593 mV for compound **5a**) as a Br atom was incorporated to the core triphenylamine. All HOMOs obtained (5.02–5.36 eV) for these compounds **1**–**6** were quite close to that (5.30 eV) of the NPD materials currently used in hole-transporting layer. Once the electrode ITO used in devices was close to 4.8 eV, then the energy barrier can be reduced. Therefore, these triphenylamines **1**–**6** prepared are potential good materials as hole-transporting materials.

3. Conclusions

A series of mesogenic derivatives based on triphenylamine were prepared and studied. The mesophases were found to be side chain dependent; compounds **1a**–**3a** with one, two, and three side chains formed lamellar columnar phases, and compounds **2b** and **3b** with four and six side chains exhibited hexagonal columnar phases. The results obtained by electrochemical and optical properties showed that these triphenylamine-based derivatives are potentially good materials to be used as hole-transporting materials.

4. Experimental section

4.1. General

All chemicals and solvents were of reagent grade obtained from Aldrich Chemical Co., and all solvents were dried by standard techniques. ^{1}H and ^{13}C NMR spectra were measured on a Bruker DRS-200. DSC thermographs were carried out on a Mettler DSC 822 and calibrated with a pure indium sample. All phase transitions are determined by a scan rate of 10.0 °C/min. Polarized optical microscopy was carried out on Zeiss Axioplan 2 equipped with a hot stage system of Mettler FP90/FP82HT. The UV–vis absorption and fluorescence spectra were obtained using a Jasco V-530 and a Hitachi F-4500 spectrometers, and all spectra were measured in CH_2Cl_2 at room temperature. Cyclic voltammetry experiments were performed with a CH Instruments model 611A electrochemical analyzer. All measurements were carried out at room temperature with a conventional three-electrode configuration consisting of a platinum working electrode, an auxiliary platinum electrode, and a nonaqueous $Ag/AgNO_3$ reference electrode. The solvent in all experiments was CH_2Cl_2, and the supporting electrolyte was 0.1 M tetrabutylammonium perchlorate. All potentials reported are referenced to an Fc^+/Fc internal standard (+0.165 V relative to the $Ag/AgNO_3$ electrode, ΔE_P=90 mV). Elemental analyses were performed on a Heraeus CHN-O-Rapid elemental analyzer. The powder diffraction data were collected from the Wiggler-A beamline of the National Synchrotron Radiation Research Center (NSRRC) with the wavelength of 1.3263 Å. Diffraction patterns were recorded in $\theta/2\theta$ geometry with step scans normally 0.02° in 2θ=1–10°/step/s and 0.05° in 2θ=10–25°/step/s and a gas flow heater was used to control the temperature. The powdered samples were charged in Lindemann capillary tubes (80 mm long and 1.0 mm thick) from Charles Supper Co. with an inner diameter of 1.0 mm. 4-Alkoxy- and 3,4-dialkoxybenzylamines, *p*,*p*′-diformyltriphenylamine, and *p*,*p*′,*p*″-triformyltriphenylamine were prepared by previously published procedures.[11,13]

4.1.1. *p*,*p*′,*p*″-Triformyltriphenylamine[11] and *p*,*p*′-diformyltriphenylamine. To a mixture of triphenylamine (20.0 g, 81.5 mmol) and dimethylformamide (80 ml) at 10 °C was dropwise added phosphoryl chloride (76 ml, 815.0 mmol) while stirring. The resulting mixture was stirred at 90–95 °C under nitrogen for 72 h. The mixture was then cooled to room temperature, poured into ice-water (1 l), and neutralized with 40% $NaOH_{(aq)}$. The brown solids were collected, washed with water, and dried. The products,

isolated as pale yellow solid, were separated and purified by column chromatography by eluting with hexane/ethyl acetate (4/1).

4.1.1.1. *p*,*p*′,*p*″-Triformyltriphenylamine. Yellow crystal, yield 10%. ^{1}H NMR ($CDCl_3$): δ 7.22 (d, J=8.6 Hz, Ar–H, 6H), 7.82 (d, J=8.6 Hz, Ar–H, 6H), 9.92 (s, –CHO, 3H). ^{13}C NMR ($CDCl_3$): δ 124.49, 131.46, 132.52, 151.14, 190.46.

4.1.1.2. *p*,*p*′-Diformyltriphenylamine. Pale yellow crystal, yield 42%. ^{1}H NMR ($CDCl_3$): δ 7.12–7.19 (m, Ar–H, 6H), 7.23–7.26 (m, Ar–H, 1H), 7.33–7.37 (m, Ar–H, 2H), 7.71–7.77 (m, Ar–H, 4H), 9.86 (s, –CHO, 2H). ^{13}C NMR ($CDCl_3$): δ 122.68, 126.20, 126.99, 130.09, 131.17, 131.24, 145.41, 151.94, 190.49.

4.1.2. 4-Hexadecyloxybenzoamine.[13] ^{1}H NMR ($CDCl_3$): 0.86 (t, J=6.4 Hz, –CH_3, 3H), 1.24–1.39 (m, –CH_2, 26H), 1.64–1.75 (m, –CH_2, 2H), 3.85 (t, J=6.5 Hz, –OCH_2, 2H), 6.58 (d, J=6.2 Hz, Ar–H, 2H), 6.70 (d, J=4.4 Hz, Ar–H, 2H).

4.1.3. 3,4-Dihexadecyloxybenzoamine.[13] ^{1}H NMR ($CDCl_3$): δ 0.85 (t, J=6.3 Hz, –CH_3, 6H), 1.26–1.79 (m, –CH_2, 56H), 3.89 (t, J=6.3 Hz, –O*C*H_2, 4H), 6.23 (d, J=4.7 Hz, Ar–*H*, 1H), 6.34 (s, Ar–*H*, 1H), 6.78 (d, J=5.7 Hz, Ar–*H*, 1H).

4.1.4. (4-Bromophenyl)-bis-(4-formylphenyl)amine. Bromine (5.3 g, 33.2 mmol) was slowly added to a solution of *p*,*p*′-diformyltriphenylamine (10.0 g, 33.2 mmol) dissolved in CH_2Cl_2 (50 ml) at 0–5 °C. After 1 h, the mixture was heated to 40 °C for 30 min. The solution was then extracted with 10% $NaHSO_{3(aq)}$, and the organic layers were combined and dried over anhydrous $MgSO_4$. The product, isolated as yellow-green solids, was obtained by recrystallization from CH_2Cl_2/CH_3OH. Yield 95%. ^{1}H NMR ($CDCl_3$): δ 7.03 (d, J=8.71 Hz, 2H), 7.15 (d, J=8.60 Hz, Ar–H, 4H), 7.46 (d, J=8.71 Hz, Ar–H, 2H), 7.75 (d, J=8.62 Hz, Ar–H, 4H), 9.86 (s, CHO). ^{13}C NMR ($CDCl_3$): δ 119.21, 123.02, 128.29, 131.31, 131.68, 133.26, 144.68, 151.60, 190.42.

4.1.5. {4-[{4-[(4-Hexadecyloxyphenylamino)methyl]-phenyl}-(4-hydroxymethylphenyl)amino]phenyl}methanol (1a, *n*=16). The mixture of *p*,*p*′,*p*″-triformyltriphenylamine (0.2 g, 0.61 mmol) and 4-hexadecycloxyphenylamine (0.41 g, 1.22 mmol) dissolved in THF (3.0 ml) was stirred at room temperature for 30 min, and then absolute ethanol (10.0 ml) and a few drops of acetic acid were added. The resulting mixture was gently heated at reflux under nitrogen for 24 h. Yellow solids were slowly precipitated upon cooling. The solids were collected, washed with methanol, and dried in vacuum. The solids (as 100% pure) and sodium borohydride (0.14 g, 3.7 mmol) were mixed and dissolved in 10 ml of THF/methanol (10/3). The resulting mixture was stirred at room temperature for 4 h. The solvent was removed under reduced pressure and the solid was extracted with CH_2Cl_2/H_2O. The product was purified by flash chromatography (silica gel) by eluting with hexane/ethyl acetate (4/1). White solid, yield 8%. ^{1}H NMR ($CDCl_3$): δ 0.87 (t, J=6.7 Hz, –CH_3, 3H), 1.25–1.41 (m, –CH_2, 26H), 1.71–1.73 (m, –CH_2, 2H), 3.86 (t, J=6.6 Hz, –OCH_2, 2H), 4.19 (s, –NCH_2, 2H), 4.60 (s, –CH_2OH, 4H), 6.61 (d, J=6.7 Hz, Ar–H, 2H), 6.77 (d, J=6.7 Hz, Ar–H, 2H), 7.00–7.04 (m, Ar–H, 6H), 7.20–7.23 (m, Ar–H, 6H). ^{13}C NMR ($CDCl_3$): δ 14.14, 22.70, 26.10, 29.37, 29.46, 29.48, 29.63, 29.69, 29.71, 31.94, 49.06, 65.02, 68.85, 114.35, 115.82, 124.28, 127.07, 128.31, 128.73, 134.02, 135.23, 142.18, 146.78, 147.29, 151.92. Anal. Calcd for $C_{43}H_{58}N_2O_3$: C, 79.34; H, 8.98; N, 4.30. Found: C, 79.25; H, 8.91; N, 4.81.

4.1.6. [4-(Bis-{4-[(4-tetradecanoxyphenylamino)methyl]-phenyl}amino)phenyl]methanol (2a, *n*=14). Off-white solid. ^{1}H NMR ($CDCl_3$): δ 0.90 (t, J=6.6 Hz, –CH_3, 6H), 1.28–1.45 (m, –CH_2, 44H), 1.73–1.76 (m, –CH_2, 4H), 3.88 (t, J=6.6 Hz, –OCH_2, 4H), 4.20 (s, –NCH_2, 4H), 4.60 (s, –CH_2OH, 2H), 6.61 (d, J=8.8 Hz, Ar–H, 4H), 6.79 (d, J=8.8 Hz, Ar–H, 4H), 7.02–7.06 (m, Ar–H, 6H), 7.21–7.23 (m, Ar–H, 6H). ^{13}C NMR ($CDCl_3$): δ 14.18, 22.74, 26.13, 29.41, 29.50, 29.52, 29.66, 29.72, 31.97, 48.99, 64.99, 68.85, 114.25, 115.83, 123.99, 124.22, 128.31, 128.70, 134.02, 135.21, 142.36, 146.83, 147.32, 151.84. Anal. Calcd for $C_{61}H_{87}N_3O_3$: C, 80.48; H, 9.63; N, 4.62. Found: C, 80.57; H, 9.90; N, 4.29.

4.1.7. [4-(Bis-{4-[(4-hexadecyloxyphenylamino)methyl]-phenyl}amino)phenyl]methanol (2a, *n*=16). White powder, yield 44%. ^{1}H NMR ($CDCl_3$): δ 0.93 (t, J=6.7 Hz, –CH_3, 6H), 1.31–1.49 (m, –CH_2, 52H), 1.75–1.80 (m, –CH_2, 4H), 3.92 (t, J=6.6 Hz, –OCH_2, 4H), 4.24 (s, –NCH_2, 4H), 4.66 (s, –CH_2OH, 2H), 6.65 (d, J=8.8 Hz, Ar–H, 4H), 6.83 (d, J=8.9 Hz, Ar–H, 4H), 7.08 (d, J=8.5 Hz, Ar–H, 6H), 7.28 (d, J=8.5 Hz, Ar–H, 6H). ^{13}C NMR ($CDCl_3$): δ 14.16, 22.73, 26.12, 29.40, 29.48, 29.51, 29.64, 29.70, 29.73, 31.96, 48.96, 65.05, 68.85, 114.19, 115.82, 123.97, 124.20, 128.30, 128.68, 134.06, 135.13, 142.40, 146.82, 147.36, 151.81. Anal. Calcd for $C_{65}H_{95}N_3O_3$: C, 80.78; H, 9.91; N, 4.35. Found C, 80.46; H, 9.86; N, 4.15.

4.1.8. [4-(Bis-{4-[(4-octadecyloxyphenylamino)methyl]-phenyl}amino)phenyl]methanol (2a, *n*=18). Off-white solid. ^{1}H NMR ($CDCl_3$): δ 0.86 (t, J=6.7 Hz, –CH_3, 6H), 1.24–1.44 (m, –CH_2, 60H), 1.69–1.75 (m, –CH_2, 4H), 3.86 (t, J=6.6 Hz, –OCH_2, 4H), 4.19 (s, –NCH_2, 4H), 4.62 (s, –CH_2OH, 2H), 6.60 (d, J=8.8 Hz, Ar–H, 4H), 6.77 (d, J=8.9 Hz, Ar–H, 4H), 7.01–7.03 (m, Ar–H, 6H), 7.21–7.23 (m, Ar–H, 6H). ^{13}C NMR ($CDCl_3$): δ 14.12, 22.70, 26.10, 29.37, 29.46, 29.48, 29.61, 29.70, 31.94, 49.02, 65.10, 68.84, 114.26, 115.81, 123.97, 124.23, 128.28, 128.70, 133.96, 135.08, 142.40, 146.82, 147.38, 151.88. Anal. Calcd for $C_{69}H_{103}N_3O_3$: C, 81.04; H, 10.15; N, 4.11. Found: C, 81.01; H, 10.76; N, 3.96.

4.1.9. [4-(Bis-{4-[(3,4-didodecanoxyphenylamino)methyl]-phenyl}amino)phenyl]methanol (2b, *n*=12). Off-white solid. ^{1}H NMR ($CDCl_3$): δ 0.94 (t, J=6.7 Hz, –CH_3, 12H), 1.31–1.33 (m, –CH_2, 72H), 1.79–1.86 (m, –CH_2, 8H), 3.94–3.99 (m, –OCH_2, 8H), 4.23 (s, –NCH_2, 4H), 4.62 (s, –CH_2OH, 2H), 6.22 (dd, J=8.5, 2.4 Hz, Ar–H, 2H), 6.32 (d, J=2.3 Hz, Ar–H, 2H), 6.83 (d, J=8.5 Hz, Ar–H, 2H), 7.06–7.10 (m, Ar–H, 6H), 7.24–7.29 (m, Ar–H, 6H). ^{13}C NMR ($CDCl_3$): δ 14.16, 22.74, 26.17, 29.42, 29.51, 29.56, 29.72, 29.76, 31.98, 48.83, 64.87, 69.11, 71.17, 101.05, 104.38, 117.63, 124.03, 124.19, 128.28, 128.74, 134.02, 135.38, 141.53, 143.76, 146.86, 147.23, 150.80. Anal. Calcd for $C_{81}H_{127}N_3O_5$: C, 79.55; H, 10.47; N, 3.44. Found: C, 79.64; H, 10.83; N, 3.17.

4.1.10. [4-(Bis-{4-[(3,4-ditetradecanoxyphenylamino)-methyl]phenyl}amino)phenyl]methanol (2b, *n*=14). Off-white solid. ^{1}H NMR ($CDCl_3$): δ 0.91 (t, J=6.5 Hz, –CH_3, 12H), 1.29–1.48 (m, –CH_2, 88H), 1.75–1.84 (m, –CH_2, 8H), 3.92–3.97 (m, –OCH_2, 8H), 4.23 (s, –NCH_2, 4H), 4.67 (s, –CH_2OH, 2H), 6.25 (s, Ar–H, 2H), 6.35 (s, Ar–H, 2H), 6.81 (d, J=8.4 Hz, Ar–H, 2H), 7.05–7.08 (m, Ar–H, 6H), 7.26–7.28 (m, Ar–H, 6H). ^{13}C NMR ($CDCl_3$): δ 14.17, 22.75, 26.17, 29.43, 29.52, 29.57, 29.73, 29.77, 31.99, 48.83, 64.85, 69.11, 71.18, 101.06, 104.39, 117.64, 124.03, 124.20, 128.28, 128.75, 134.01, 135.40, 141.53, 143.76, 146.87, 147.21, 150.80. Anal. Calcd for $C_{89}H_{143}N_3O_5$: C, 80.07; H, 10.80; N, 3.15. Found: C, 79.47; H, 10.45; N, 2.68.

4.1.11. [4-(Bis-{4-[(3,4-dihexadecyloxyphenylamino)-methyl]phenyl}amino)phenyl]methanol (2b, *n*=16). Off-white solid. ^{1}H NMR ($CDCl_3$): δ 0.86 (t, J=6.6 Hz, –CH_3, 12H), 1.24–1.43 (m, –CH_2, 104H), 1.71–1.77 (m, –CH_2, 8H), 3.87–3.92 (m, –OCH_2, 8H), 4.18 (s, –NCH_2, 4H), 4.62 (s, –CH_2OH, 2H), 6.17 (dd, J=8.5, 2.1 Hz, Ar–H, 2H), 6.27 (d, J=2.0 Hz, Ar–H, 2H), 6.76 (d, J=8.5 Hz, Ar–H, 2H), 7.01–7.04 (m, Ar–H, 6H), 7.21–7.23 (m, Ar–H, 6H). ^{13}C NMR ($CDCl_3$): δ 14.11, 22.69, 26.11, 29.37, 29.46, 29.52, 29.67, 29.72, 31.94, 48.92, 65.08, 69.09, 71.10, 101.05, 104.38, 117.51, 124.00, 124.21, 128.28, 128.78, 133.71, 135.14, 141.49, 143.72, 146.86, 147.34, 150.76. Anal. Calcd for $C_{97}H_{159}N_3O_5$: C, 80.50; H, 11.07; N, 2.90. Found: C, 80.05; H, 10.93; N, 2.69.

4.1.12. Tris-{4-[(4-tetradecanoxyphenylamino)methyl]-phenyl}amine (3a, *n*=14). ^{1}H NMR ($CDCl_3$): δ 0.96 (t, J=6.1 Hz, –CH_3, 9H), 1.35–1.51 (m, –CH_2, 66H), 1.82 (m, –CH_2, 6H), 3.94 (t, J=6.1 Hz, –OCH_2, 6H), 4.26 (s, –NCH_2, 6H), 6.67 (d, J=8.6 Hz, Ar–H, 4H), 6.84–6.86 (m, Ar–H, 6H), 7.10–7.11 (m, Ar–H, 6H), 7.29–7.30 (m, Ar–H, 6H). ^{13}C NMR ($CDCl_3$): δ 14.19, 22.77, 26.17, 29.44, 29.55, 29.69, 29.76, 32.00, 48.93, 68.84, 114.14, 115.84, 124.17, 128.67, 134.05, 142.51, 146.90, 151.79. Anal. Calcd for $C_{81}H_{120}N_4O_3$: C, 81.22; H, 10.10; N, 4.68. Found: C, 80.78; H, 10.29; N, 4.51.

4.1.13. Tris-{4-[(4-hexadecyloxyphenylamino)methyl]-phenyl}amine (3a, *n*=16). Off-white powder, yield 19%. ^{1}H NMR ($CDCl_3$): δ 0.86 (t, J=6.6 Hz, –CH_3, 9H), 1.24–1.43 (m, –CH_2, 78H), 1.69–1.75 (m, –CH_2, 6H), 3.86 (t, J=6.6 Hz, –OCH_2, 6H), 4.19 (s, –NCH_2, 6H), 6.62 (d, J=8.7 Hz, Ar–H, 6H), 6.77 (d, J=8.7 Hz, Ar–H, 6H), 7.01 (d, J=8.1 Hz, Ar–H, 6H), 7.22 (d, J=8.3 Hz, Ar–H, 6H). ^{13}C NMR ($CDCl_3$): δ 14.07, 22.67, 26.08, 29.34, 29.44, 29.48, 29.60, 29.68, 31.91, 49.23, 68.87, 114.58, 115.85, 124.13, 128.76, 133.63, 142.07, 146.91, 152.13. Anal. Calcd for $C_{87}H_{132}N_4O_3$: C, 81.51; H, 10.38; N, 4.37. Found: C, 81.55; H, 10.45; N, 4.34.

4.1.14. Tris-{4-[(4-octadecyloxyphenylamino)methyl]-phenyl}amine (3a, *n*=18). ^{1}H NMR ($CDCl_3$): δ 0.86 (t, J=6.7 Hz, –CH_3, 9H), 1.28–1.42 (m, –CH_2, 90H), 1.69–1.75 (m, –CH_2, 6H), 3.86 (t, J=6.6 Hz, –OCH_2, 6H), 4.19 (s, –NCH_2, 6H), 6.61 (d, J=8.4 Hz, Ar–H, 6H), 6.76 (d, J=8.4 Hz, Ar–H, 6H), 7.01 (d, J=8.4 Hz, Ar–H, 6H), 7.22 (d, J=8.4 Hz, Ar–H, 6H). ^{13}C NMR ($CDCl_3$): δ 14.10, 22.68, 26.09, 29.35, 29.48, 29.60, 29.67, 29.69, 31.93, 49.14, 68.85, 114.43, 115.82, 124.13, 128.73, 133.71, 142.04, 146.89, 152.00. Anal. Calcd for $C_{93}H_{144}N_4O_3$: C, 81.76; H, 10.62; N, 4.10. Found: C, 81.58; H, 10.89; N, 3.78.

4.1.15. Tris-{4-[(3,4-didecanoxyphenylamino)methyl]-phenyl}amine (3b, *n*=10). ^{1}H NMR ($CDCl_3$): δ 0.94 (t, J=6.6 Hz, –CH_3, 18H), 1.33–1.51 (m, –CH_2, 84H), 1.78–1.87 (m, –CH_2, 12H), 3.86 (m, –OCH_2, 12H), 4.25 (s, –NCH_2, 6H), 6.23 (dd, J=8.4, 2.3 Hz, Ar–H, 3H), 6.33 (d, J=2.0 Hz, Ar–H, 3H), 6.84 (d, J=8.5 Hz, Ar–H, 3H), 7.09 (d, J=8.3 Hz, Ar–H, 6H), 7.29 (d, J=8.3 Hz, Ar–H, 6H). ^{13}C NMR ($CDCl_3$): δ 14.17, 22.74, 26.15, 29.42, 29.50, 29.66, 29.72, 31.97, 48.84, 69.06, 71.29, 100.94, 104.27, 117.54, 124.16, 128.74, 133.91, 141.52, 143.69, 146.91, 150.78. Anal. Calcd for $C_{99}H_{156}N_4O_6$: C, 79.36; H, 10.49; N, 3.74. Found: C, 79.53; H, 10.57; N, 3.44.

4.1.16. Tris-{4-[(3,4-didodecanoxyphenylamino)methyl]-phenyl}amine (3b, *n*=12). ^{1}H NMR ($CDCl_3$): δ 0.87 (t, J=6.6 Hz, –CH_3, 18H), 1.25–1.44 (m, –CH_2, 108H), 1.72–1.79 (m, –CH_2, 12H), 3.88–3.93 (m, –OCH_2, 12H), 4.19 (s, –NCH_2, 6H), 6.18 (dd, J=8.5, 2.4 Hz, Ar–H, 3H), 6.28 (d, J=2.4 Hz, Ar–H, 3H), 6.77 (d, J=8.6 Hz, Ar–H, 3H), 7.02 (d, J=8.4 Hz, Ar–H, 6H), 7.23 (d, J=8.4 Hz, Ar–H, 6H). ^{13}C NMR ($CDCl_3$): δ 14.13, 22.70, 26.11, 29.38, 29.46, 29.52, 29.62, 29.68, 31.94, 48.86, 69.07, 71.12, 100.96, 104.29, 117.54, 124.14, 128.74, 133.85, 141.54, 146.90, 150.76. Anal. Calcd for $C_{111}H_{180}N_4O_6$: C, 79.99; H, 10.89; N, 3.36. Found: C, 79.70; H, 10.77; N, 3.24.

4.1.17. Tris-{4-[(3,4-ditetradecanoxyphenylamino)-methyl]phenyl}amine (3b, *n*=14). ^{1}H NMR ($CDCl_3$): δ 0.94 (t, J=6.4 Hz, –CH_3, 18H), 1.32–1.51 (m, –CH_2, 132H), 1.79–1.87 (m, –CH_2, 12H), 3.94–3.99 (m, –OCH_2, 12H), 4.25 (s, –NCH_2, 6H), 6.22 (dd, J=8.5, 2.1 Hz, Ar–H, 3H), 6.33 (d, J=2.0 Hz, Ar–H, 3H), 6.83 (d, J=8.5 Hz, Ar–H, 3H), 7.09 (d, J=8.3 Hz, Ar–H, 6H), 7.29 (d, J=8.3 Hz, Ar–H, 6H). ^{13}C NMR ($CDCl_3$): δ 14.07, 22.65, 26.06, 29.33, 29.42, 29.47, 29.63, 29.68, 31.89, 48.74, 68.97, 71.03, 100.84, 104.15, 117.47, 124.06, 128.64, 133.83, 141.42, 143.64, 146.82, 150.70. Anal. Calcd for $C_{123}H_{204}N_4O_6$: C, 80.51; H, 11.21; N, 3.05. Found C, 80.07; H, 11.52; N, 2.66.

4.1.18. Tris-{4-[(3,4-dihexadecyloxyphenylamino)-methyl]phenyl}amine (3b, *n*=16). ^{1}H NMR ($CDCl_3$): δ 0.87 (t, J=6.1 Hz, –CH_3, 18H), 1.25–1.43 (m, –CH_2, 156H), 1.71–1.80 (m, –CH_2, 12H), 3.87–3.93 (m, –OCH_2, 12H), 4.18 (s, –NCH_2, 6H), 6.17 (dd, J=8.3, 2.1 Hz, 3H), 6.26 (d, J=2.0 Hz, Ar–H, 3H), 6.77 (d, J=8.4 Hz, Ar–H, 3H), 7.02 (d, J=8.3 Hz, Ar–H, 6H), 7.23 (d, J=8.3 Hz, Ar–H, 6H). ^{13}C NMR ($CDCl_3$): δ 14.13, 22.71, 26.12, 29.48, 29.53, 29.69, 29.74, 31.95, 48.85, 69.08, 71.13, 100.96, 104.28, 117.57, 124.14, 127.74, 133.87, 141.55, 143.70, 146.91, 150.79. Anal. Calcd for $C_{135}H_{228}N_4O_6$: C, 80.94; H, 11.47; N, 2.80. Found: C, 80.44; H, 11.36; N, 2.60.

4.1.19. Tris-{4-[2-(4-hexadecyloxyphenyl)vinyl]phenyl}-amine (4a, *n*=16). The mixture of (4-methoxybenzyl)-triphenylphosphonium bromide (1.3 g, 1.93 mmol) and

potassium *tert*-butoxide (0.26 g, 2.32 mmol) dissolved in dry THF (10 ml) was stirred at room temperature for 15 min and then *p*,*p*′,*p*″-triformyltriphenylamine (0.2 g, 0.61 mmol) was slowly added. The mixture was refluxed for 48 h. The solution was concentrated and then extracted with CH_2Cl_2/H_2O. The organic layers were collected and dried over anhydrous $MgSO_4$. The product was purified by flash chromatography (silica gel) by eluting with hexane/ethyl acetate (8/1). Yellow solid, yield 19%. ^{1}H NMR ($CDCl_3$): δ 0.86 (t, J=6.6 Hz, –CH_3, 9H), 1.24–1.45 (m, –CH_2, 84H), 1.74–1.79 (m, –CH_2, 6H), 3.95 (t, J=6.6 Hz, OCH_2, 6H), 6.85–6.97 (m, Ar–H, 13H), 7.02–7.07 (m, Ar–H, 7H), 7.35–7.47 (m, Ar–H, 10H). ^{13}C NMR ($CDCl_3$): δ 14.12, 22.69, 26.05, 29.29, 29.37, 29.41, 29.58, 29.60, 29.67, 29.70, 31.93, 68.11, 114.73, 124.22, 125.88, 127.02, 127.11, 127.50, 130.18, 132.49, 146.42, 158.75. Anal. Calcd for $C_{90}H_{129}NO_3$: C, 84.92; H, 10.21; N, 1.10. Found: C, 83.93; H, 9.51; N, 0.95.

4.1.20. Bis-{4-[(4-hexadecyloxyphenylamino)methyl]-phenyl}amine (5a, *n*=16). White powder, yield 77%. ^{1}H NMR ($CDCl_3$): δ 0.89 (t, J=6.1 Hz, –CH_3, 6H), 1.27–1.44 (m, –CH_2, 52H), 1.73–1.75 (m, –CH_2, 4H), 3.88 (t, J=6.1 Hz, –OCH_2, 4H), 4.20 (s, –NCH_2, 4H), 6.60–6.63 (m, Ar–H, 4H), 6.79 (d, J=8.0 Hz, Ar–H, 4H), 6.98–7.08 (m, Ar–H, 7H), 7.22–7.24 (m, Ar–H, 6H). ^{13}C NMR ($CDCl_3$): δ 14.09, 22.69, 26.11, 29.36, 29.46, 29.51, 29.62, 29.70, 31.94, 49.03, 68.91, 114.23, 115.90, 122.75, 124.12, 124.20, 128.64, 129.23, 133.97, 142.43, 146.97, 147.82, 151.89. Anal. Calcd for $C_{64}H_{93}N_3O_2$: C, 82.09; H, 10.01; N, 4.49. Found: C, 81.95; H, 10.16; N, 4.32.

4.1.21. Bis-{4-[(3,4-dihexadecyloxyphenylamino)-methyl]phenyl}amine (5b, *n*=16). White powder, yield 75%. ^{1}H NMR (500 MHz, $CDCl_3$): δ 0.91 (t, J=6.7 Hz, –CH_3, 12H), 1.29–1.51 (m, –CH_2, 104H), 1.75–1.84 (m, –CH_2, 8H), 3.92–3.96 (m, –OCH_2, 8H), 4.23 (s, –NCH_2, 4H), 6.27 (dd, J=8.5 Hz, 2.1 Hz, 2H), 6.35 (d, J=2.0 Hz, Ar–H, 2H), 6.81 (d, J=8.5 Hz, Ar–H, 2H), 7.02–7.09 (m, Ar–H, 7H), 7.25–7.29 (m, Ar–H, 6H). ^{13}C NMR ($CDCl_3$): δ 14.06, 22.66, 26.09, 29.34, 29.43, 29.49, 29.59, 29.67, 31.92, 49.01, 68.90, 71.01, 100.96, 104.28, 117.57, 122.74, 124.10, 124.18, 128.61, 129.22, 133.95, 142.42, 143.70, 146.94, 147.79, 150.79. Anal. Calcd for $C_{96}H_{157}N_3O_4$: C, 81.35; H, 11.17; N, 2.96. Found: C, 81.63; H, 11.19; N, 2.97.

4.1.22. (4-Bromophenyl)-bis-{4-[(4-hexadecyloxyphenyl-amino)methyl]phenyl}amine (6a, *n*=16). White powder, yield 59%. ^{1}H NMR ($CDCl_3$): δ 0.93 (t, J=6.7 Hz, –CH_3, 6H), 1.31–1.49 (m, –CH_2, 52H), 1.75–1.80 (m, –CH_2, 4H), 3.92 (t, J=6.6 Hz, –OCH_2, 4H), 4.25 (s, –NCH_2, 4H), 6.65 (d, J=8.8 Hz, Ar–H, 4H), 6.83 (d, J=8.9 Hz, Ar–H, 4H), 6.97 (d, J=8.9 Hz, Ar–H, 2H), 7.07 (d, J=8.4 Hz, Ar–H, 4H), 7.29 (m, J=8.4 Hz, Ar–H, 4H), 7.35 (m, J=8.8 Hz, Ar–H, 2H). ^{13}C NMR ($CDCl_3$): δ 14.16, 22.72, 26.12, 29.39, 29.48, 29.50, 29.64, 29.70, 29.73, 31.96, 48.90, 68.83, 114.15, 115.81, 124.46, 125.00, 128.75, 132.18, 134.60, 142.36, 146.41, 146.96, 151.82. Anal. Calcd for $C_{64}H_{92}N_3O_2Br$: C, 75.71; H, 9.13; N, 4.14. Found: C, 75.90; H, 9.32; N, 3.93.

Acknowledgements

We thank the National Science Council of Taiwan, ROC for funding (NSC 95-2752-M-008-010-PAE) in generous support of this work.

References and notes

1. (a) *Handbook of Liquid Crystals*; Demus, D., Goodby, J., Gray, G. W., Spiess, H. W., Vill, V., Eds.; Wiley-VCH: Weinheim, 1998; Vol. 2a; (b) Hudson, S. A.; Maitlis, P. M. *Chem. Rev.* **1993**, *93*, 861–885; (c) Espinet, P.; Esteruelas, M. A.; Oro, L. A.; Serrano, J. L.; Sola, E. *Coord. Chem. Rev.* **1992**, *117*, 215–274; (d) Maitlis, P.; Giroud-Godquin, A. M. *Angew. Chem., Int. Ed. Engl.* **1991**, *30*, 375–402; (e) Serrano, J. L. *Metallomesogens: Synthesis, Properties, and Applications*; VCH: New York, NY, 1996.
2. (a) Chien, C. W.; Liu, K. T.; Lai, C. K. *J. Mater. Chem.* **2003**, *13*, 1588–1595; (b) Lai, C. K.; Tsai, C. H.; Pang, Y. S. *J. Mater. Chem.* **1998**, *8*, 1355–1360.
3. Craats, A. M.; Warman, J. M.; Müllen, K.; Geerts, Y.; Brand, J. *Adv. Mater.* **1998**, *10*, 36–38.
4. (a) Baldo, M. A.; O'Brien, D. F.; You, Y.; Shoustikov, A.; Sibley, S.; Thompson, M. E.; Forrest, S. R. *Nature* **1998**, *395*, 151–154; (b) Tamayo, A. B.; Alleyne, B. D.; Djurovich, P. I.; Lamansky, S.; Tsyba, I.; Ho, N. N.; Bau, R.; Thompson, M. E. *J. Am. Chem. Soc.* **2003**, *125*, 7377–7387; (c) Lee, M. T.; Liao, C. H.; Tsai, C. H.; Chen, C. H. *Adv. Mater.* **2005**, *17*, 2493–2497.
5. (a) Schmidt-Mende, L.; Fechtenkotter, A.; Mullen, K.; Moons, E.; Friend, R. H.; MacKenzie, J. D. *Science* **2001**, *293*, 1119–1122; (b) Kawamoto, M.; Mochizuki, H.; Shishido, A.; Tsutsumi, O.; Ikeda, T.; Lee, B.; Shirota, Y. *J. Phys. Chem. B* **2003**, *107*, 4887–4893.
6. (a) van de Crats, A. M.; Warman, J. M.; Fechtenkotter, A.; Brand, J. D.; Harbison, M. A.; Müllen, K. *Adv. Mater.* **1999**, *11*, 1469–1472; (b) Hanna, J.; Kogo, K.; Kafuku, K. EP-A 0915144, 1999; (c) Adam, D.; Closs, F.; Frey, T.; Funhoff, D.; Haarer, D.; Ringsdorf, H.; Schumacher, P.; Siemensmeyer, K. *Phys. Rev. Lett.* **1993**, *70*, 457–460.
7. (a) Adam, D.; Schuhmacher, P.; Simmerer, J.; Haüssling, L.; Paulus, W.; Siemensmeyer, K.; Etzbach, K. H.; Ringsdorf, H.; Haarer, D. *Adv. Mater.* **1995**, *7*, 276–280; (b) Simmerer, J.; Glüsen, B.; Paulus, W.; Kettner, A.; Schuhmacher, P.; Adam, D.; Etzbach, K. H.; Siesmensmeyer, J.; Wendorff, J. H.; Ringsdorf, H.; Haarer, D. *Adv. Mater.* **1996**, *8*, 815–819; (c) Christ, T.; Glüsen, B.; Greiner, A.; Kettner, A.; Sander, R.; Stümpflen, V.; Tsukruk, V.; Wendorff, J. H. *Adv. Mater.* **1997**, *9*, 48–52.
8. (a) Liu, C. K.; Fechtenkötter, A.; Watson, M. D.; Müllen, K.; Bard, A. J. *Chem. Mater.* **2003**, *15*, 124–130; (b) Mochizuki, H.; Hasui, T.; Kawamoto, M.; Ikeda, T.; Adachi, C.; Taniguchi, Y.; Shirota, Y. *Macromolecules* **2003**, *36*, 3457–3464; (c) Kestemont, G.; Halleux, V. D.; Lehmann, M.; Ivanov, D. A.; Watsonc, M.; Geerts, Y. H. *Chem. Commun.* **2001**, 2074–2075; (d) Mochizuki, H.; Hasui, T.; Kawamoto, M.; Shiono, T.; Ikeda, T.; Adachi, C.; Taniguchib, Y.; Shirotac, Y. *Chem. Commun.* **2000**, 1923–1924; (e) Tokuhisa, H.; Era, M.; Tsutsuia, T. *Appl. Phys. Lett.* **1998**, *72*, 2639–2641.
9. (a) Wu, I. Y.; Lin, J. T.; Tao, Y. T.; Balasubramaniam, E. *Adv. Mater.* **2000**, *12*, 668–669; (b) Tao, Y. T.; Chuen, C. H.;

Ko, C. W.; Peng, J. W. *Chem. Mater.* **2002**, *14*, 4256–4261; (c) Casalbore-Miceli, G.; Esposti, A. D.; Fattori, V.; Marconi, G.; Sabatini, C. *Phys. Chem. Chem. Phys.* **2004**, *6*, 3092–3096.
10. Lin, B. C.; Cheng, C. P.; Ping, Z.; Lao, M. *J. Phys. Chem. A* **2003**, *107*, 5241–5251.
11. Lai, G.; Bu, X. R.; Santos, J.; Mintz, E. *Synlett* **1997**, 1275–1276.
12. *Modern Molecular Photochemistry*; Turro, N. J., Ed.; Benjamin/Cummings: Menlo Park, CA, 1978.
13. Lai, C. K.; Chang, C. H.; Tsai, C. H. *J. Mater. Chem.* **1998**, *8*, 599–602.